Demonstrating Cost Effective Thermal Energy Storage in Molten Salts: DLR's TESIS Test Facility

Christian Odenthal[1], Freerk Klasing[1] and Thomas Bauer[1]

[1] *German Aerospace Center (DLR), Linder Höhe, 51147 Cologne, Germany*

Abstract

The present paper gives an overview of a new test facility for molten salt thermocline storage systems and components, which is currently being constructed at DLR in Cologne. The paper also presents DLR thermocline-filler modelling and the potential of the novel storage technology compared to the two-tank state of the art molten salt storage. In this work, an extensive parametric study is combined with an optimization routine. The approach allows a better comparison since it finds only those storage configurations, which can directly substitute the two-tank system in a given power plant. Results show that, compared to the two-tank molten salt system, the thermocline technology achieves high exergetic efficiency at only slightly increased storage volume size and a huge decrease in salt inventory.

Introduction

Storing thermal energy in liquid molten salts provides an easy to handle and cost effective solution for thermal energy storage at high temperatures. The technology offers great potential for the energy transition in Germany. Examples are the improved use of waste heat from industrial processes or increasing the flexibility of power stations and cogeneration, as well as the conversion and storage of fluctuating surplus electricity from renewable energy sources.

Proven technology, low cost salts as storage materials, excellent heat transfer rates and operation at ambient pressure are some of the key attributes for molten salt technology. By embedding a low cost solid filler material into the molten salt storage tank, further cost reductions of up to 33 % can be achieved [1]. The thermocline concept with filler has already been demonstrated in a large scale of 170 MWh_{th} at the SolarOne power plant [2]. This system used thermal oil as HTF and rocks as filler material. Experimental results with molten salt, but in a smaller scale of 2.3 MWh_{th} have been presented by Sandia [3]. A mid-sized experiment with 3 m height, 1 m diameter and thermal oil operating at up to 350 °C has been investigated at CEA [4]. CEA has also successfully demonstrated a complete plant, consisting of a fresnel collector, an organic rankine cycle (ORC) and a thermocline thermal storage [5].

However, new technological challenges arise, mainly from chemical side reactions and the necessity in finding optimized operation strategies for such highly dynamic systems. At CIEMAT simplified models for system simulations [6] and possible operation strategies [7] have been theoretically investigated. An analytic model developed at EEWRC has been used for the application of sensivity analysis for thermocline optimization [8].

Overview of the TESIS Test Facility

At DLR in cologne a large scale *Test facility for thermal Energy Storage In molten Salts* (TESIS) is currently being set up and expected to be operational by mid-2017.

The facility comprises of two independent test facilities, namely TESIS:store and TESIS:com, as shown in Fig. 1 (a) and (b), respectively. Key component of the TESIS:store facility is a thermocline tank which can be equipped with or without a filler material, whilst the TESIS:com facility has a special test section where various components such as heat exchangers, absorber tubes, valves, measurement equipment, etc. can be tested. Both facilities use a hot and a cold reservoir tank, which

act as a heat source or sink as shown in Fig. 1 as well. Vast reductions in energy consumption are achieved by using these reservoirs instead of high power thermal heaters and coolers.

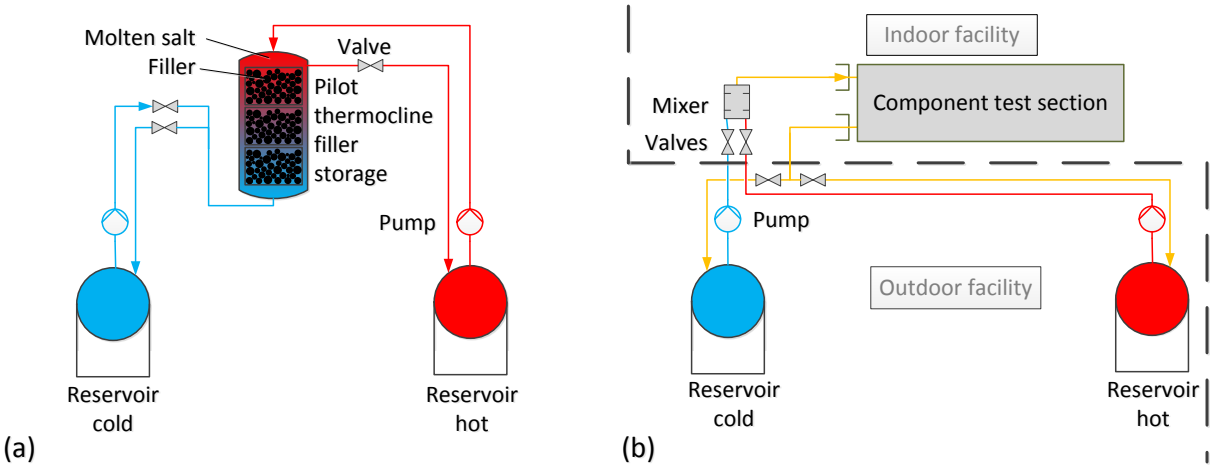

Fig. 1: Working principle of the TESIS test facilities: (a) TESIS:store for testing thermocline storage systems; (b) TESIS:com for component tests

The following sections give a more detailed insight into both parts of the TESIS test facility.

TESIS:store Test Facility for Testing Thermocline Storage Technology

The TESIS:store facility's storage volume is illustrated in an cross sectional view and a photo of the actual plant in Fig. 2. The volume of the tank is 22 m³ and can be equipped with three equally sized baskets, holding the filler material. The key parameters of the facility are summarized in Table 1.

During charging, hot salt inflows at the top of the storage volume and moves through the filler material. In the picture, the upper part of the storage volume is already heated to the maximum temperature (red color). When the salt reaches the part of the storage volume which is still at the lower temperature (blue color), heat is transferred from the hotter salt to the colder filler material. In this region, a thermocline zone develops, where the temperature gradually drops, as indicated by the purple color. The cooled salt eventually leaves the storage volume at the bottom, returning to the cold reservoir. For the discharging process, the process is reversed, with salt from the cold reservoir inflowing at the bottom of the storage tank. The heated salt then leaves the tank through the pipe at the top of the packing material, returning to the hot tank.

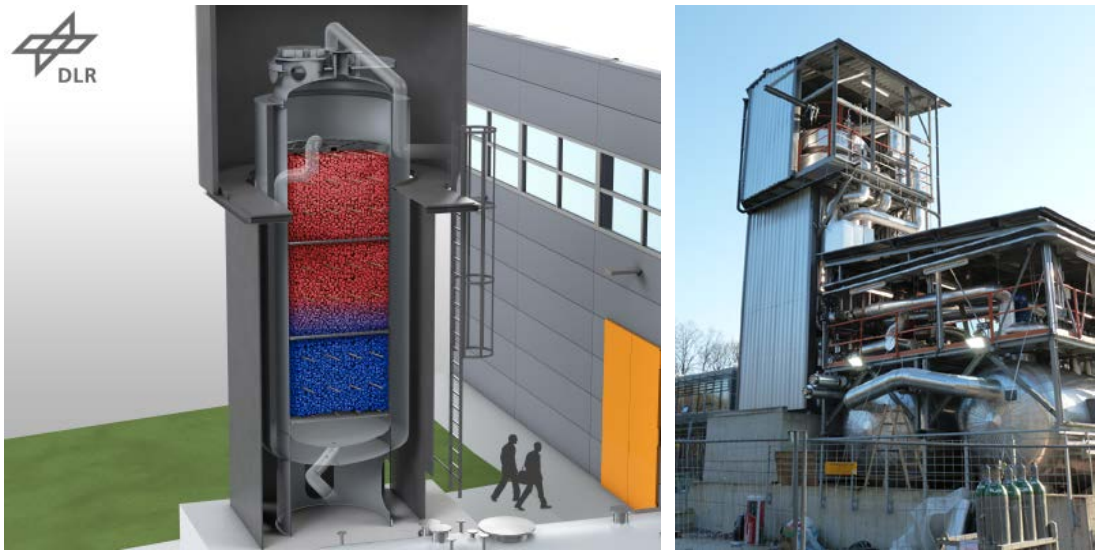

Fig. 2: Cross-sectional view of the TESIS:store thermocline test facility (left) and photo of the actual plant (right)

Due to its large size, it is possible to study the dynamic behavior of the storage system and minimize side effects, which usually affect smaller lab scale experiments. Furthermore, the experimental results help refining DLR's inhouse computer models to optimize simulations on the larger system scale. By analyzing the storage materials of the test facility regularly, further insight into filler and molten salt chemistry on the large scale is achieved.

TESIS:com Test Facility for Component Tests

The TESIS:com test facility, specifically designed for component tests, is shown in Fig. 3, alongside with a photo of the test section. Currently, a dummy tube is attached for the commissioning, which will be replaced by the test equipment in the future. The facility is provided with hot and cold molten salt from its reservoir tanks situated at the outside of the building. Contrary to the TESIS:store facility, it is possible to supply the test section with molten salt from both reservoirs simultaneously at any mixing ratio. This enables various testing scenarios. For example, it is possible extract a large amount of heat from the hot salt with a heat exchanger, or to cycle through extreme temperature gradients of up to 50 Kelvin/s. Furthermore, long term testing is also possible, due to the embedded electrical flow heater with 420 kW thermal power.

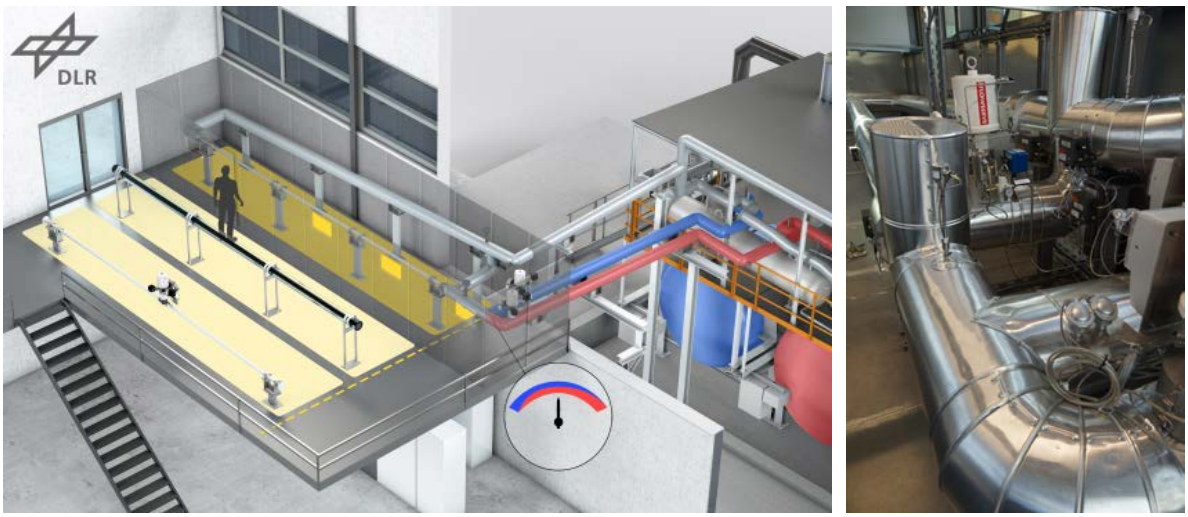

Fig. 3: View from the inside of the TESIS:com test facility (left) and photo from the test section with dummy tube for commissioning (right)

The TESIS:com facility allows DLR and its industrial partners accelerating market entry of newly developed equipment. Key parameters of the TESIS:com facility are summarized in Table 1.

Table 1: Key parameters of the TESIS test facility

Parameter	TESIS:store	TESIS:com	Unit
Molten salt medium	Nitrate - Nitrite salt mixtures		-
Max. operation temperature	560		°C
Min. operation temperature	150		°C
Max. thermal gradient	-	50	K/s
Mass flow rate	4	8	kg/s
Heating power *	115	420	kW
Cooling power	420	420	kW

** Total electrical heating power of TESIS is around 1150 kW including auxiliary and tank heaters*

In the next chapter, the potential for thermocline storage on the large scale for a parabolic trough power plant with 100 MW_{el} power is discussed.

Thermocline performance on the large scale

Computer Model

To model the thermocline storage, a computer model is implemented which is based on the partial differential equations (PDE) of the fluid and solid temperature fields.

As for the fluid, the transient term for the change in inner energy, the transport of thermal energy, the conduction of thermal energy within the bed and the coupling with the solid are taken into account. When considering large storage volumes, heat losses can be neglected, since their influence is comparatively small.

The fluid PDE then reads

$$\varepsilon\rho_{\mathrm{f}}c_{\mathrm{f}}\frac{\partial T_{\mathrm{f}}}{\partial t} = -\rho_{\mathrm{f}}c_{\mathrm{f}}v_{0,\mathrm{x,f}}\frac{\partial T_{\mathrm{f}}}{\partial x} + \lambda_{\mathrm{eff,x,sf}}\frac{\partial^2 T_{\mathrm{f}}}{\partial x^2} + \dot{Q}_f{}''' \tag{1}$$

Here, ε denotes the porosity, $\rho_{\mathrm{f}}c_{\mathrm{f}}$ the volumetric heat capacity of the fluid, $v_{0,\mathrm{x,f}}$ the superficial flow velocity of the fluid and $\dot{Q}_f{}'''$ the energy transfer from or to the solid. $\lambda_{\mathrm{eff,x,sf}}$ is the effective heat conductivity of the bed filled with salt. The effective conductivity of the solid and fluid can be considered as a parallel interconnection of their resistances, weighted by the respective porosities. Hence, the effective conductivity is

$$\lambda_{\mathrm{eff,x,sf}} = \left(\frac{\varepsilon}{\lambda_{\mathrm{f}}} + \frac{1-\varepsilon}{\lambda_{\mathrm{s}}}\right)^{-1}. \tag{2}$$

In terms of the solid, there is only the transient change in inner energy and a coupling term with the fluid, hence the solid PDE reads

$$(1-\varepsilon)\rho_{\mathrm{s}}c_{\mathrm{s}}\frac{\partial T_{\mathrm{s}}}{\partial t} = \dot{Q}_{\mathrm{s}}{}'''. \tag{3}$$

The product $\rho_{\mathrm{s}}c_{\mathrm{s}}$ is the volumetric heat capacity of the solid and $\dot{Q}_{\mathrm{s}}{}'''$ the coupling term, which is calculated from

$$\dot{Q}_f{}''' = -\dot{Q}_s{}''' = k_{\mathrm{vol}} \cdot (T_{\mathrm{s}} - T_{\mathrm{f}}),$$

$$\text{where } k_{\mathrm{vol}} = \frac{1}{\alpha_{\mathrm{vol}}} + \frac{2\lambda}{5 \cdot d_{\mathrm{part}}} \tag{4}$$

is the effective heat transfer coefficient. The second term in k_{vol} takes the resistance arising from the conductivity of the solid λ into account and has been developed by Schmidt & Willmott [9].

The film heat transfer α_{vol} coefficient is calculated from a Nusselt-correlation derived by Wakao et al. [10]:

$$Nu = 2 + 1.1 \cdot Pr^{\frac{1}{3}} \cdot Re_{\mathrm{part,PB}}^{0,6} = \frac{a_{\mathrm{v}} \cdot \alpha_{\mathrm{vol}} \cdot d_{\mathrm{part}}}{\lambda_{\mathrm{f}}} = \frac{6(1-\varepsilon) \cdot \alpha_{\mathrm{vol}}}{\lambda_{\mathrm{f}}}. \tag{5}$$

The specific surface per volume a_{v} is calculated from the porosity ε and the average particle diameter d_{part}

$$a_{\mathrm{v}} = \frac{6(1-\varepsilon)}{d_{\mathrm{part}}} \tag{6}$$

The pressure loss is calculated from Ergun's [11] equation, with the bed length L_{stor} and the dynamic viscosity of the fluid μ_{f}:

$$\Delta p = \frac{L_{\mathrm{stor}}}{d_{\mathrm{part}}} \frac{(1-\varepsilon)}{\varepsilon^3} \left(\frac{150 \cdot (1-\varepsilon) \cdot \mu_{\mathrm{f}}}{\rho_{\mathrm{f}} v_{0,x,\mathrm{f}} \cdot d_{\mathrm{part}}} + 1{,}75 \right) \rho_{\mathrm{f}} v_{0,\mathrm{f}}^2 \tag{7}$$

To solve the PDEs, a spatial discretization is applied, leading to a set of ordinary differential equations (ODEs), which are discretized by the "theta-rule" with respect to time. This leads to a system of linear dependent equations which can be described by

$$(\bar{\bar{\boldsymbol{I}}} + \vartheta \cdot \bar{\bar{\boldsymbol{M}}}^{\mathbf{n+1}}) \cdot \boldsymbol{T}^{\mathbf{n+1}} = \left(\bar{\bar{\boldsymbol{I}}} - (1-\vartheta) \cdot \bar{\bar{\boldsymbol{M}}}^{\mathbf{n}}\right) \cdot \boldsymbol{T}^{\mathbf{n}} + \boldsymbol{b}. \tag{8}$$

$\bar{\bar{\boldsymbol{I}}}$ is the identity matrix, $\bar{\bar{\boldsymbol{M}}}^{\mathbf{n+1}}$ and $\bar{\bar{\boldsymbol{M}}}^{\mathbf{n}}$ are sparse band matrices, $\boldsymbol{T}^{\mathbf{n+1}}$ and $\boldsymbol{T}^{\mathbf{n}}$ the vectors of the temperature field for the next and current time step, respectively, whilst vector $\boldsymbol{b}$ contains the boundary conditions. The scalar ϑ determines the weighting between implicit and explicit time discretization. For the current study it is set to $\vartheta = 0.5$, which corresponds to the Crank-Nicholson scheme. The linear system is solved by the Matlab® routine mldivide which is part of a DLR in-house tool for sizing regenerator type thermal energy storages.

Parametric Study of a Large Scale Thermocline System

With the prescribed model a parametric study is carried out. For the study a thermocline storage volume with Solarsalt as HTF and basalt rocks as filler is considered. For the attached process, a parabolic trough thermal power plant with 235 MW_{th} nominal thermal power and a corresponding mass flow rate of $\dot{m}_{\mathrm{f}} = 581.85\ \mathrm{kg/s}$ is considered. The storage time during charging ($t'_{\mathrm{e,set}}$) is fixed to 12 hours. The superscript $'$ generally indicates the charging cycle, whereas $''$ the discharging cycle. The input values for the simulation are summarized in Table 2.

As main parameters, the permitted change in exit temperature (ΔT_{e}), cross-sectional area (A_0), particle diameter (d_{part}) and porosity (ε) are varied. For a mono-disperse packing, a porosity of 40 % can be achieved. By mixing different particle sizes, the porosity can be further reduced [12]. However, in this case pressure loss correlations and thermal models must be adopted accordingly. Since the model is only capable to account for mono-disperse packings, a fictional packing with 30 % porosity and only little deviation from realistic results is assumed. A maximum permitted pressure drop (Δp_{max}) of 0.5 bar for the bed is assumed. Finally, the length of the storage volume (L_{stor}) is subject to optimization for the emerging combinations of input parameters. All parameters are given in Table 2 as well.

Table 2: Input values for parametric study

Description	Value	Unit
Storage material	Basalt	-
Heat transfer fluid (HTF)	Solarsalt	-
Storage time ($t'_{\mathrm{e,set}}$)	12	h
Thermal power ($\dot{Q}_{\mathrm{th}}$)	235	MW_{th}
Mass flow ($\dot{m}_{\mathrm{f}}$)	581.85	kg/s
Nominal inlet temperature ($T'_{\mathrm{in,nom}}$)	550	°C
Nominal outlet temperature ($T''_{\mathrm{in,nom}}$)	290	°C
Flow length (L_{stor})	Variable	m
Permitted change in exit temperature (ΔT_{e})	10 – 70	K
Cross-sectional area (A_0)	200 – 6000	m^2
Particle diameter (d_{part})	1 – 50	mm
Porosity (ε)	30; 40	%
Permitted pressure loss (Δp_{max})	0.5	bar

To find the necessary storage length for a given set of input parameters, the model is coupled with an optimization routine. The optimization routine adopts the storage length in a way that the storage time

during charging ($t'_{\mathrm{e,set}} = 12h = const$) is exactly met when the permitted change in exit temperature (ΔT_{e}) is reached. An illustration of the scheme is shown in Fig. 4.

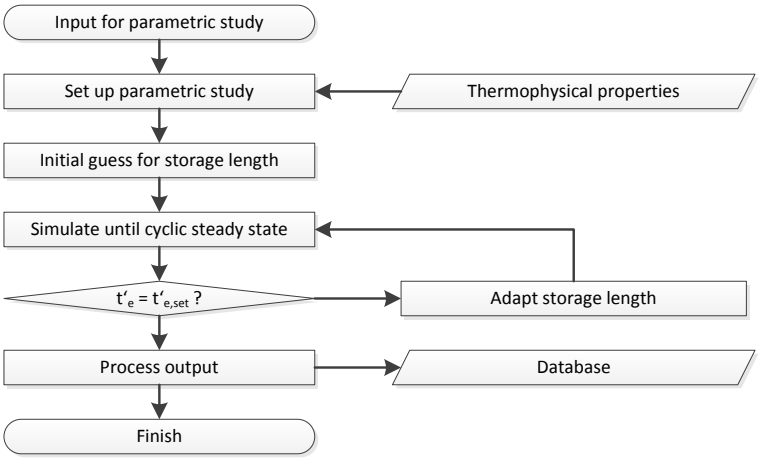

Fig. 4: Simplified scheme of the sizing tool

The methodology of adjusting the storage time for each configuration allows a straightforward comparison among each other, since every configuration now could be substituted with an existing two-tank molten salt storage system, having the same charging time (t'_{e}). Finally, a suitable quantity for the rating is necessary, which is described in the next section.

Exergetic Rating of Storage Volumes

The rating methodology is based on an exergetic efficiency which can be considered as an exergy regaining factor Ξ. Under nominal conditions (derived from the power cycle), a specific exergy stream $\dot{E}'_{\mathrm{nom}}$ during the charging time t'_{e} is available. The resulting nominal exergy $\Delta E'_{\mathrm{stor,nom}}$ is fed into the storage volume and results in an extracted exergy $\Delta E''_{\mathrm{stor}}$ after discharging, as shown in Fig. 5.

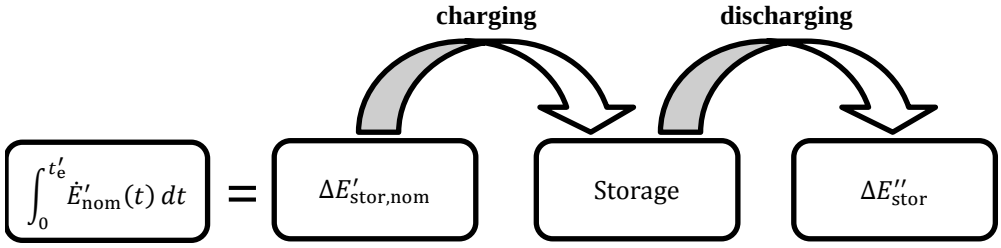

Fig. 5: Exergetic quantities for the rating of the storage volume

The exergy regaining factor Ξ is then simply the quotient of extracted exergy $\Delta E''_{\mathrm{stor}}$ and the nominal exergy $\Delta E'_{\mathrm{stor,nom}}$, as given by the following equation:

$$\Xi = \frac{\Delta E''_{\mathrm{stor}}}{\Delta E'_{\mathrm{stor,nom}}}$$

$$= \frac{\int_0^{t''_{\mathrm{e}}} \dot{m}'' \cdot \left[h\left(T''_{\mathrm{in,nom}}\right) - h\left(T''_{\mathrm{out}}(t)\right) - T_{\mathrm{u}} \cdot \left(s\left(T''_{\mathrm{in,nom}}\right) - s\left(T''_{\mathrm{out}}(t)\right)\right)\right] dt}{\int_0^{t'_{\mathrm{e}}} \dot{m}' \cdot \left[h\left(T'_{\mathrm{in,nom}}\right) - h\left(T'_{\mathrm{out,nom}}\right) - T_{\mathrm{u}} \cdot \left(s\left(T'_{\mathrm{in,nom}}\right) - s\left(T'_{\mathrm{out,nom}}\right)\right)\right] dt}. \quad (9)$$

In the equation, h denotes the specific enthalpy, s the specific entropy with 25°C as reference temperature und T_{u} the ambient temperature.

To contrast the exergy regaining factor Ξ, a second rating quantity is necessary. Due to the high share of the total costs caused by the molten salt [13], the total mass of the salt is considered here.

Results of the Parametric Study

In total 770 simulations are carried out, with the four parameters (ΔT_e, A_0, d_{part}, ε) shown in Table 2 being varied. From the data the following conclusions can be drawn:

- Configurations with the lowest necessary fluid mass also have the highest exergy regain.
- Optimum cross sectional areas lie around 200 m² to 600 m².
- The optimum particle diameter is about 2 mm in most cases.
- Permitted change in exit temperature has a significant impact on utilization, as stated in an earlier publication [14].
- A lower porosity appears clearly advantageous in terms of fluid holdup with only very little decline in exergy regain.

Table 3 shows the impact of the two parameters porosity and permitted change in exit temperature. Table 3 shows selected results for optimized storage configurations in terms of exergy regain Ξ where A_0 and d_{part} are optimized. The values are rounded to fit into the table. For comparison, the data of a two-tank molten salt storage system (2-T) is given as well.

Table 3: Optimum storage configurations for 30 % and 40 % porosity and permitted change in exit temperature between 10 K and 70 K. Two-tank molten salt storage for comparison.

System	**TC, $\varepsilon = 30\%$**				**TC, $\varepsilon = 40\%$**				**2-T**	**-**
Permitted change in exit temperature (ΔT_e)	**10**	**30**	**50**	**70**	**10**	**30**	**50**	**70**	**0**	**K**
Exergy regain (Ξ)	99.8	99.8	99.7	99.6	99.8	99.8	99.7	99.6	100	%
Storage length (L_{stor})	41.9	25.0	36.4	35.9	82.4	37.3	72.9	71.8	34.2	m
Cross-sectional area (A_0)	400	600	400	400	200	400	200	200	400	m²
Storage volume (V_{stor})	16.8	15.0	14.6	14.3	16.5	14.9	14.6	14.4	13.7	10^3m³
Particle diameter (d_{part})	2	2	2	2	2	1	2	2	-	mm
Pressure loss (Δp_f)	381	150	331	327	483	416	427	421	-	mbar
Fluid mass (m_f)	9.2	8.2	8.0	7.9	12.0	10.9	10.6	10.5	25.1	kt
Solid mass (m_s)	35.1	31.4	30.5	30.1	29.6	26.8	26.2	25.8	0.0	kt
LD storage (L_{stor}/D_{stor})	1.86	0.90	1.61	1.59	5.16	1.65	4.57	4.50	1.51	-

First, it can be seen that all configurations reach very high exergy regain rates. The reason for that is because pressure losses as well as driving temperature differences between molten salt and particles are very small. Due to the latter effect, the thermocline zone also remains very narrow, which causes exergy losses due to the temperature drop only at the very end of the cycles.

Since the two-tank system has no temperature differences and change in exit temperature, the exergy regain is 100 %. When compared to this, the thermocline with filler performs still very well. Due to the lower utilization, the thermocline storage volume is larger than the two-tank system. However, the increase in size lies between 5 % and 20 %, mainly depending on the permitted change in exit temperature. When comparing the necessary fluid mass, the thermocline outperforms the two-tank system by a factor of roughly 2 – 3. If the porosity can be further reduced, the necessary fluid mass could be further reduced.

Summary

In this work, a summary of DLR's new component and thermocline storage test facilities, namely TESIS:com and TESIS:store were given. The commissioning is on schedule and both facilities are expected to be fully operational by mid-2017.

The exergetic rating in the present study shows, that the thermocline filler storage causes only minor losses in exergy of less than half a percent when compared to the two-tank molten salt storage system. Simultaneously, the indicators for future investment costs are very promising: The tank size increases only by 5 to 20 percent, whilst the amount of salt is decreased by a factor between 2 – 3. These results were calculated under the assumption of constant boundary conditions from both power block and solar field. Further studies with detailed computer models of these components would allow a further refinement of the results.

Acknowledgements

The authors thank the German Federal Ministry for Economic Affairs and Energy for the financial support given for this work in the MS-STORE project (Contract No. 0325497 A).

Literature

[1] C. Libby, “Solar Thermocline Storage Systems: Preliminary Design Study,” 2010.
[2] S. E. Faas, L. R. Thorne, and N. D. Fuchs, E.A. ; Gilbertsen, “10 MWe Solar Thermal Central Receiver Pilot Plant: Thermal Storage Subsystem Evaluation Final report,” 1986.
[3] J. E. Pacheco, S. K. Showalter, and W. J. Kolb, “Development of a Molten-Salt Thermocline Thermal Storage System for Parabolic Trough Plants,” *J. Sol. Energy Eng.*, vol. 124, no. 2, p. 153, 2002.
[4] A. Bruch, J. F. Fourmigué, and R. Couturier, “Experimental and numerical investigation of a pilot-scale thermal oil packed bed thermal storage system for CSP power plant,” *Sol. Energy*, vol. 105, pp. 116–125, 2014.
[5] S. Rodat, A. Bruch, N. Dupassieux, and N. El Mourchid, “Unique Fresnel Demonstrator Including ORC and Thermocline Direct Thermal Storage: Operating Experience,” *Energy Procedia*, vol. 69, pp. 1667–1675, 2015.
[6] R. Bayón and E. Rojas, “Analytical function describing the behaviour of a thermocline storage tank: A requirement for annual simulations of solar thermal power plants,” *Int. J. Heat Mass Transf.*, vol. 68, pp. 641–648, Jan. 2014.
[7] M. Biencinto, R. Bayón, E. Rojas, and L. González, “Simulation and assessment of operation strategies for solar thermal power plants with a thermocline storage tank,” *Sol. Energy*, vol. 103, pp. 456–472, 2014.
[8] A. M. Bonanos and E. V. Votyakov, “Sensitivity analysis for thermocline thermal storage tank design,” *Renew. Energy*, vol. 99, pp. 764–771, 2016.
[9] F. W. Schmidt and A. J. Willmott, *Thermal energy storage and regeneration*, 1st ed. Washington, D.C., USA: Hemisphere Publishing Corporation, 1981.
[10] N. Wakao and S. Kagei, *Heat and mass transfer in packed beds*. New York: Gordon and Breach Science Publishers Inc., 1982.
[11] S. Ergun and a. a. Orning, “Fluid Flow through Randomly Packed Columns and Fluidized Beds,” *Ind. Eng. Chem.*, vol. 41, no. 6, pp. 1179–1184, Jun. 1949.
[12] J. Latham, A. Munjiza, and Y. Lu, “On the prediction of void porosity and packing of rock particulates,” vol. 125, pp. 10–27, 2002.
[13] B. Kelly and D. Kearney, “Thermal Storage Commercial Plant Design Study for a 2-Tank Indirect Molten Salt System,” National Renewable Energy Laboratory (NREL), 2004.
[14] C. Odenthal, N. Breidenbach, and T. Bauer, “Modelling and Operation Strategies of DLR’s Large Scale Thermocline Test Facility (TESIS),” *Am. J. Phys.*, 2017.